Astron. Astrophys. 274, 662–666 (1993)

ASTRONOMY AND ASTROPHYSICS

# Accurate wavelengths of near infrared coronal lines from spectroscopic measurements of NGC 6302⋆

**M. Reconditi**[1] **and E. Oliva**[2]

[1] Università degli Studi di Firenze, Dip. di Astronomia e Scienza dello Spazio, Largo E.Fermi 5, I-50125 Firenze, Italy
[2] Osservatorio Astrofisico di Arcetri, Largo E.Fermi 5, I-50125 Firenze, Italy

Received February 23, accepted March 16, 1993

**Abstract.** The wavelengths of forbidden lines from [Mg VIII], [Si VI], [Si VII], [S VIII] and [Ca VIII] have been determined to an accuracy of 15 km/s on the basis of optical and near infrared spectra of the high excitation planetary nebula NGC 6302 where these lines are prominent and free from blending. The new wavelengths are much more accurate than those so far available and could be useful for the study of the coronal line region in Seyfert galaxies.

**Key words:** atomic and molecular data – infrared radiation – lines: identification – spectroscopy

## 1. Introduction

Coronal lines are forbidden transitions from highly ionized species ($h\nu_{ion} > 100$ eV) which take their names from the fact that they were first observed in the solar corona. In the optical range the most famous one is probably [Fe XIV] $\lambda$5303.4 – the green coronal line – which, together with [Fe X] $\lambda$6374.5, have been extensively used to study the solar corona (e.g. Jefferies et al. 1971; Magnant-Crifo 1973; Chandrasekhar et al. 1991)

Due to the great difficulty to produce in the laboratory sufficient amounts of coronal ions, virtually all the information concerning the wavelengths of their forbidden transitions are based on solar observations and are mostly limited to $\lambda < 9000$ Å. A summary of the coronal lines observed in the sun is given in Svensson et al. (1974); see also Jefferies et al. (1971) and Magnant-Crifo (1973). A practical list of forbidden line wavelengths is given by Kaufman & Sugar (1986). Detailed information for transitions from highly ionized stages of potassium through nickel can be also found in Sugar & Corliss (1985), Martin et al. (1988) and Fuhr et al. (1988). While the optical lines are relatively well studied, the only coronal lines in the infrared ($\lambda > 9000$ Å) with accurate wavelengths are those of [Fe XIII] ($\lambda\lambda$10746.8, 10797.9).

*Send offprint requests to*: E. Oliva

⋆ Based on observations collected at the European Southern Observatory, La Silla, Chile

Coronal lines are often found in the spectra of active galaxy nuclei (AGNs) and originate in the so called 'coronal line region' (CLR) whose physical conditions – temperature, density, size, origin of the ionization – are still poorly known and much debated (e.g. Oke & Sargent 1968; Penston et al. 1984; Veilleux 1988; Korista & Ferland 1989; Contini & Viegas 1992). In the optical one finds the well known transitions of iron ions, namely [Fe VII] $\lambda$6087.0, [Fe X] $\lambda$6374.5, [Fe XI] $\lambda$7891.8, which appear as relatively faint emission features ($\lesssim$5% of H$\alpha$) in the observed spectra. In the near infrared [Si VI] ($\simeq$1.962 $\mu m$) and [Si VII] ($\simeq$2.48 $\mu m$) are among the strongest emission lines measured in the Seyfert galaxy NGC 1068 (Oliva & Moorwood 1990; Moorwood & Oliva 1991) and there is also evidence that [Ca VIII] ($\simeq$2.32 $\mu m$) may be present (Moorwood & Oliva 1992).

In NGC 4151 Osterbrock et al. (1990) reported the detection of a line at 9911.4 Å which they ascribe to [S VIII] though prudently commenting that the 'identification is plausible but more speculative'. Indeed, using the wavelength of [S VIII] given in Svensson et al. (1974) – 9911 Å– one would conclude that the [S VIII] line in NGC 4151 is red-shifted with respect to the other lines in the spectrum whilst [Fe X] and [Fe XI] are blue-shifted, a fact which seems to be a common characteristic for the coronal lines in AGNs (Penston et al. 1984).

The rest wavelengths of [Si VI], [Si VII] and [Ca VIII] are badly known: $\delta\lambda \gtrsim 20$ Å, equivalent to an error of about 300 km/s (Ashley & Hyland 1988, hereafter AH88) and barely enough to guaranty a reasonable line identification.

The ideal astrophysical laboratory for the determination of line wavelengths are planetary nebulae because their spectra are rich of prominent and narrow lines from ions covering a wide range of ionization degrees. It is for this reason that most of the information on the positions of forbidden lines are based on careful spectroscopic studies of planetary nebulae (Bowen 1955, 1960; see also Kaler et al. 1976). To study coronal lines one needs to find an extreme PN with a very high ionization degree, we have chosen NGC 6302 which is already known to exhibit prominent lines of [Si VI] and [Si VII] (AH88). The data are described in Sect. 2 and the results are presented in Sect. 3.

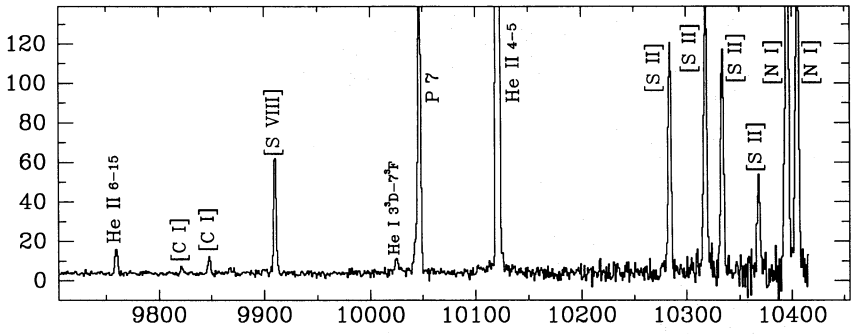


**Fig. 1.** Portion of the EMMI spectrum of NGC 6302 including the [S VIII] line. Wavelengths are in Å and the flux scale is in units of $10^{-15}$ erg cm$^{-2}$ s$^{-1}$ Å$^{-1}$

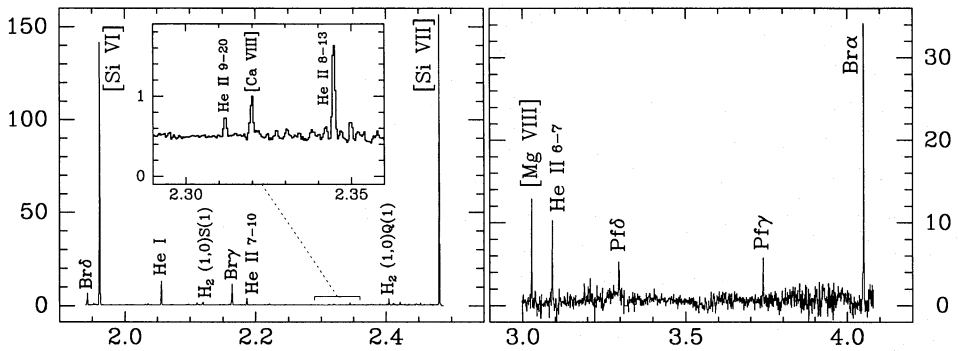


**Fig. 2.** IRSPEC spectra of NGC 6302 including coronal lines. Wavelengths are in $\mu$m and the flux scale is in units of $10^{-10}$ erg cm$^{-2}$ s$^{-1}$ $\mu$m$^{-1}$

## 2. The observational data

A 4200–10500 Å spectrum was obtained in April 1991 using the red arm of the multimode ESO instrument (EMMI, Dekker et al. 1986) on the ESO-NTT telescope. The detector was a 2024x2024 Ford-Aereospace CCD with a projected pixel size of 0.35 arcsec, the slit width was 1.5 arcsec. The dispersion from the 600 grooves/mm grating used in first order was $\simeq$0.8 Å/pixel and 5 exposures at different grating angles were needed to cover the whole wavelength range. At $\lambda > 7000$ Å a cut-on filter was used to prevent order overlapping, integration time was 1000 sec per each long slit frame. A portion of the final 1D spectrum extracted from the central 7 arcsec, centered at 10100 Å and including the line of [S VIII] is displayed in Fig. 1.

The infrared spectra were collected during two observing runs (April 1991, September 1992) at the ESO-NTT telescope using the IRSPEC infrared spectrometer (Moorwood et al. 1991) equipped with a SBRC 62x58 InSb array and using two interchangeable gratings with 300 and 600 grooves/mm and respectively optimized for observations at $\lambda \geq 3\ \mu m$ and $\lambda \lesssim 2.5\ \mu m$. The pixel size was 2.2 arc-sec along the slit and $\simeq$5 Å ($\simeq$10 Å at $\lambda \geq 3\ \mu m$) along dispersion. At each wavelength (grating position) we alternated one or two object and sky (5' E) measurements each lasting 2 minutes. Selected sections of the spectrum including the coronal lines of interest are shown in Fig. 2.

A full description of data acquisition and reduction – all performed using MIDAS (the ESO reduction package) and fitting Gaussians to determine the central position of the lines – are given in Reconditi (1992) and will be reported in a forthcoming paper dedicated to a detailed analysis of the data. For the purpose of this work we just describe in some details the procedures used for the accurate determination of wavelengths.

– Optical data.

The wavelength vs. pixel dispersion was first determined in the classical way from measurements of an Ar discharge lamp taken at the end of the night, a fit with a second degree polynom yielded r.m.s scatters of $\simeq$0.1 pixels. The calibration was then checked using the numerous sky lines (Osterbrock & Martel 1992) in the long slit frames of NGC 6302 and corrected for the small shifts ($\lesssim$ 1 pixel) which occurred between the astronomical and calibration exposures. The final accuracy on the sky lines was comparable to that found for Ar lines and always $< 0.3$ pixels.

– Infrared data.

For wavelengths up to 2.3 $\mu m$ (i.e. for the [Si VI] measurements) we used the numerous OH sky lines in the airglow spectrum (Oliva & Origlia 1992) which were clearly visible both on the 'object' and 'sky' frames. At longer wavelengths we used measurements of a Ne lamp taken immediately before (after) the object and without moving the grating. The mechanical stability of the grating was checked on many object–sky pairs taken at wavelengths with strong OH lines and found to be always better than 0.05 pixels over times $> 10$ minutes and longer than those elapsed between the object and Ne frames. The wavelength dispersion on the small (62 pixels) array of IRSPEC is linear within a negligible fraction of a pixel and the pixel size $\Delta\lambda_P$ is directly related to the central wavelength of the frame (i.e. the grating angle) by the expression for the grating dispersion

$$\Delta\lambda_P = \frac{\alpha_P \cos\gamma_0}{d^{-1}m}\sqrt{1-\left(\frac{m\lambda_c}{2d\cos\gamma_0}\right)^2} = C_1\sqrt{1-\left(\frac{m\lambda_c}{C_2}\right)^2}$$

where $m$ is the grating order, $d$ is the groove spacing, $\gamma_0$ is the off-axis angle, * $\alpha_P$ is the angle projected by a pixel onto the grating and $\lambda_c$ is the central wavelength of the frame (i.e. that falling on pixel 31.5); note that the term under square root effectively is the cosine of the grating angle. The numerical values of $C_1$ and $C_2$ – namely $C_1$=12.39 Å, $C_2$=6.572 $\mu m$ for grating #1 (that used at $\lambda \geq 3$ $\mu m$) and $C_1$=6.197 Å, $C_2$=3.286 $\mu m$ for grating #2 (used at shorter wavelengths) – were derived from least square fits of the values of $\Delta\lambda_P$ measured in frames containing two or more reference lines (Ne, Kr, OH) and spanning all the range of grating angles allowed by the instrument, the r.m.s. scatter of the fits was 0.07 pixels. Adopting Eq. 1 – which is used in the IRSPEC context of MIDAS for the wavelength calibration – we could calibrate spectra to an accuracy of $\simeq 0.1$ pixels even using a single reference line.

Since the lines under consideration lie at wavelengths where the atmospheric transmission is quite bad we were concerned about the possibility that this could introduce systematic errors in the determination of line wavelengths. For this reason we repeated the measurements at different times in order to have the object – which lies close to the plane of the ecliptic – at as different as possible relative velocities ($\Delta v_{helio}$) with respect to the earth, the heliocentric corrections at the two epochs were +18 and –29 km/s. The shift in velocity produced dramatic variations in the intensities of [Si VI] (an effect already reported by AH88) and [Ca VIII], but virtually no change in their heliocentric wavelengths. For [Si VII] we also found that its central positions reproduced within better than 15 km/s (the practical limit of the data) whilst the wavelengths of [Mg VIII] suffered by slightly larger errors (±25 km/s).

The variation of line fluxes with $\Delta v_{helio}$ is related to the fact that the atmospheric absorption is produced by features which are much narrower than the instrumental resolution.

This effect can be visualized in Fig. 3 where we give the positions of [Ca VIII] and [Si VI] onto a high resolution spectrum of the atmospheric transmission (adapted from Hall 1970). When the heliocentric correction is zero (i.e. when the radial component of the earth motion toward the object is null) the lines are shifted from their rest wavelengths by –38 km/s, the heliocentric velocity of NGC 6302 (Minkowski & Johnson 1967). At this position both [Si VI] and [Ca VIII] lie at wavelengths where the atmospheric transmission is quite good (cf. Fig. 3). When we observed the object in april 1991 the earth was moving toward NGC 6302 by 18 km/s (i.e. $\Delta v_{helio}$=18 km/s) and the lines were blue-shifted into regions of even better telluric transmission. In september 1992, on the contrary, the earth was moving 29 km/s away from the object and the lines were red-shifted at wavelengths were the atmospheric transmission is very bad, and this explains why both [Si VI] and [Ca VIII] were found much fainter (a factor of ~4 and ~2, respectively) at this epoch. The presence of such an effect in the data can be therefore used both to infer that the coronal lines in NGC 6302 are very narrow (< 30 km/s,

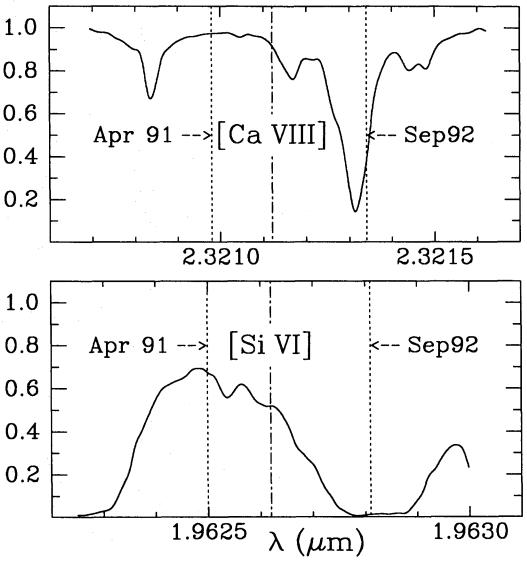


**Fig. 3.** Traces of the atmospheric transmission adapted from Hall (1970). The dot-dashed lines give the heliocentric positions of the [Ca VIII] and [Si VI] transitions in NGC 6302 (–38 km/s from their rest wavelengths given in Table 1). The dotted lines indicate the wavelengths at which the lines were shifted by the motion of the earth at the epochs of observations. The wavelength ranges in the two figures correspond to about 2 pixels of IRSPEC, see Sect. 2 for more details

see also AH88) and as a further check on the accuracy of the measured wavelengths.

## 3. Results

The spectra shown in Figs. 1, 2 refer to the central 7 arcsec (along the slit) of the nebula, all lines are unresolved and no dynamical motion inside the source are visible inside this region (see also Minkowski & Johnson 1967). One therefore expects that the wavelength accuracy for bright and isolated lines should be comparable to that obtained for the reference lines (lamps and/or sky) and $\lesssim 0.3$ pixels. This is indeed confirmed by the fact that the wavelengths of lines with well known rest positions – H I, He I, He II, [O I], [O III], [N II], $H_2$ and many others – were found to reproduce within the above mentioned error.

This result can be visualized in Fig. 4 where we plot the measured heliocentric positions of ~ 100 lines. All the points referring to transitions with precise $\lambda_0$ lie within ±15 km/s from –38 km/s – the nominal velocity of the source (cf. Minkowski & Johnson 1967) – and with an r.m.s. scatter of about 6 km/s.

The lines from low (e.g. [O I], [C I], $H_2$) and high (He II, [Ar V]) ionization species have the same velocities relative to us, hence there is no evidence of important bulk motions between regions with different ionization degrees in the central part of the source. A more definite check in this respect would be measuring coronal lines with well known positions, but this is unfortunately impossible as the lines of [Fe X] and [Fe XI] – ions with ionization potentials intermediate between [Si VI] and [S VIII] – are not detected to a level of $10^{-3}$ of the strength of

* The dispersion equation is valid for 'Littrow' spectrometers – such as IRSPEC – where the off-axis angle of the grating is perpendicular to the dispersion direction

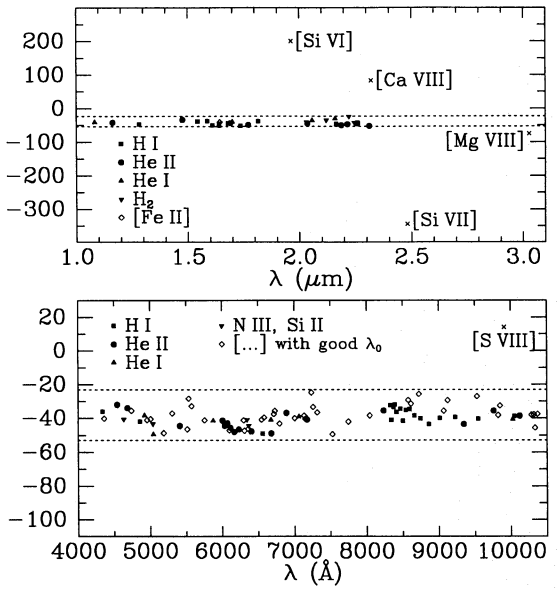


**Fig. 4.** Measured positions $v/c = (\lambda - \lambda_0)/\lambda_0$ of optical (bottom) and infrared (top) lines. The velocities ($y$-axis) are in km/s while the horizontal lines ($\pm$15 km/s from the systemic velocity of NGC 6302, -38 km/s) are plotted to better visualize the scatter of the data. The lines for which we give improved rest wavelengths ($\lambda_0$) are indicated by crosses

[Si VI]. Indeed, this is a surprising and puzzling result which indicates that the Fe/Si relative abundance in the 'coronal' gas is 3 orders of magnitudes below the solar value! We will return on this problem in a forthcoming paper. Under the very reasonable assumption that the highly ionized gas does not have any bulk motion with respect to lower excitation regions one can determine the rest positions of the newly measured coronal lines by simply red-shifting of 38 km/s – the radial motion of the source – the measured wavelengths. The results are listed in Table 1 where we also include two other lines for which we found that our wavelengths were more precise than those available in the literature. The errors were conservatively assumed to be $\pm$15 km/s – the maximum scatter of the data in Fig. 4 – except for the [Mg VIII] line for which we found a larger difference (25 km/s) between measurements taken at different epochs (cf. Sect. 2). In the case of [Si VI], [Si VII] and [Ca VIII] the new positions are a factor $\sim$ 20 more precise than those so far available.

With the new wavelengths one finds that the line at $\lambda$ = 9911.4 Å in the spectrum of the Seyfert 1 galaxy NGC 4151 (cf. Table 3 of Osterbrock et al. 1990) is blue-shifted with respect to the rest position of [S VIII] by 40 km/s. This fact supports its identification as [S VIII] because the coronal lines of [Fe XI] and [Fe X] are also blue-shifted by similar amounts (cf. Penston et al. 1984; Osterbrock et al. 1990). In the Seyfert 2 galaxy NGC 1068 the measured rest position of [Si VI] is 19615 Å (Oliva & Moorwood 1990) which implies a blue-shift of $\simeq$ 200 km/s and compatible within the errors with that derived by Penston et al. (1984) from the [Fe X] line.

**Table 1.** Rest wavelengths and wavenumbers.

| Ion | Transition ($l$–$u$) | $\lambda_{air}$ (Å) | $\nu_{vac}$ (cm$^{-1}$) |
|---|---|---|---|
| [Mg VIII] | $2p\ ^2P^o_{1/2}$–$^2P^o_{3/2}$ | 30271.3 $\pm$ 2.5 | 3302.56 $\pm$ .27 |
| [Si VII] | $2p^4\ ^3P_2$–$^3P_1$ | 24826.6 $\pm$ 1.2 | 4026.84 $\pm$ .20 |
| [Ca VIII] | $3p\ ^2P^o_{1/2}$–$^2P^o_{3/2}$ | 23214.1 $\pm$ 1.2 | 4306.55 $\pm$ .20 |
| [Si VI] | $2p^5\ ^2P^o_{3/2}$–$^2P^o_{1/2}$ | 19628.7 $\pm$ 1.0 | 5093.19 $\pm$ .25 |
| [S VIII] | $2p^5\ ^2P^o_{3/2}$–$^2P^o_{1/2}$ | 9912.72 $\pm$ .50 | 10085.3 $\pm$ 0.5 |

## 4. Conclusions

We have used high quality optical and infrared spectra of the high excitation planetary nebula NGC 6302 to derive accurate central positions of coronal lines ([Si VI], [Si VII], [S VIII], [Ca VIII], [Mg VIII]). The new wavelengths are up to a factor of 20 more accurate than those previously available and could be useful for the study of the coronal line region in AGNs.

*Acknowledgements.* This paper is based on a part of the thesis work by M. Reconditi. We are grateful to an anonymous referee for a very quick answer and for helpful comments.

## References

Ashley M.C.B., Hyland A.R., 1988, ApJ 331, 532 (AH88)
Bowen I.S., 1955, ApJ 121, 306
Bowen I.S., 1960, ApJ 132, 1
Chandrasekhar T., Desai J.N., Ashok N.M., Pasacheff J.M., 1991, Solar Phys. 131, 25
Contini M., Viegas S.M., 1992, ApJ 401, 481
Dekker H., Delabre B., D'Odorico S., 1986, SPIE Instrum. in Astronomy 6 vol. 627, 339
Fuhr J.R., Martin G.A., Wiese W.L., 1988, J. Phys. Chem. Ref. Data 17, Suppl. 4
Hall D.N.B., 1970, *An Atlas of Infrared Spectra of the Solar Photosphere and of Sunspot Umbrae*, Tucson: Kitt Peak National Observatory
Korista K.T., Ferland G.J., 1989, ApJ 343, 678
Jefferies J.T., Orrall F.Q., Zirker J.B., 1971, Solar Phys. 16, 103
Kaler J.B., Aller L.H., Czyzak S.J., Epps H.W., 1976, ApJS 31, 163
Kaufman V., Sugar J., 1986, J. Phys. Chem. Ref. Data 15, 321
Magnant-Crifo F., 1973, Solar Phys. 34, 173
Martin G.A., Fuhr J.R., Wiese W.L., 1988, J. Phys. Chem. Ref. Data 17, Suppl. 3
Minkowski R., Johnson H.M., 1967, ApJ 148, 659
Moorwood A.F.M., Moneti A., Gredel R., 1991, The Messenger 63, 77
Moorwood A.F.M., Oliva E., 1991, The Messenger 63, 57
Moorwood A.F.M., Oliva E., 1992, *Near IR spectroscopy of active and starburst nuclei*, Astronomical IR Spectroscopy Conference, Calgary June 92, in press.
Oke J.B., Sargent W.L.W., 1968, ApJ 151, 807
Oliva E., Moorwood A.F.M., 1990, ApJL 348, L5
Oliva E., Origlia L., 1992, A&A 254, 466

Osterbrock D.E., Shaw R.A., Veilleux S., 1990, ApJ 352, 561

Osterbrock D.E., Martel A., 1992, P.A.S.P. 104, 76

Penston M.V., Fosbury R.A.E., Boksenberg A., Ward M.J., Wilson A.S., 1984, MNRAS 208, 347

Reconditi M., 1992, Thesis, University of Florence.

Sugar J., Corliss C., 1985, J. Phys. Chem. Ref. Data 14, Suppl. 2

Svensson L.A., Ekberg J.O., Edlen B., 1974, Solar Phys. 34, 173

Veilleux S., 1988, AJ 95, 1695

This article was processed by the author using Springer-Verlag TEX A&A macro package 1992.